Feasibility of using the P-Cable high-resolution 3D seismic system in detecting and monitoring CO_2 leakage

Malin Waage[1], Sunny Singhroha[1], Stefan Bünz[1], Kate A. Waghorn[1], Benjamin Bellwald[2], Sverre Planke[2,3,4]

1- CAGE-Centre for Arctic Gas Hydrate, Environment, and Climate, Department of Geosciences, UiT The Arctic University of Norway, N-9037 Tromsø, Norway

2- Volcanic Basin Petroleum Research (VBPR) AS, Høienhald, Blindernveien 5, 0361 Oslo, Norway

3- Centre for Earth Evolution and Dynamics (CEED), University of Oslo, Sem Sælands vei 1, N-0371 Oslo, Norway

4- Research Centre for Arctic Petroleum Exploration (ARCEx), UiT The Arctic University of Norway, Tromsø, Norway

Keywords: 4D seismic, high-resolution, P-Cable

Abstract

The P-Cable technology is an acquisition principle for high-resolution and ultra-high-resolution 3D seismic data. Many 3D seismic data sets have been acquired over the last decade, but the application in time-lapse studies for monitoring of CO_2 storage is a new and forthcoming topic. High-resolution 3D (HR3D) seismic has the potential to detect and monitor CO_2 leakage at carbon capture and storage (CCS) sites with higher accuracy at depths shallower than ~1-2 km below the seafloor compared to more traditional conventional seismic time-lapse data. Here, we synthesize and evaluate research related to detection of subsurface CO_2 movement using the P-Cable system and address the comparative advantages and disadvantages of conventional and HR3D technologies for subsurface fluid migration monitoring. The studies that exist on P-Cable time-lapse seismic data present good repeatability, comparable to conventional 4D seismic data, indicating promising future monitoring potential. Analysis of detection limits of CO_2 on P-Cable 4D seismic data from the Snøhvit CO_2 storage site in the Barents Sea show the ability to detect very small amounts of CO_2 (1.3-10.6 tonnes; 3.3-27.4% gas saturation depending on the fluid distribution) in the shallow subsurface (~500 m below the seafloor). These detection limits are one to two orders of magnitude better than the detection limits of conventional seismic data at similar depths. We conclude that the P-Cable acquisition system can be a valuable monitoring tool in detecting small leakages and can complement conventional seismic data monitoring of the deeper interval (injection and storage zones).

Introduction: The application of 4D seismic as a fluid monitoring tool

Carbon Capture and Storage (CCS) is recognized as a crucial mitigation technology in limiting global warming to 2°C (Masson-Delmotte et al., 2018), and accurate monitoring strategies aid safe and efficient operations. The integrity of the rock sealing a CO_2 storage formation has a crucial role in determining how much and how quickly CO_2 leaks back into the hydrosphere and atmosphere. A highly effective subsurface fluid trap (or seal) can impede fluid migration indefinitely (until all CO2 has transformed into carbonate minerals after several thousands of years and is securely trapped (Alcalde et al., 2018)), however geologic processes, including increased fluid input and tectonic deformation, can alter the subsurface conditions sufficiently to allow previously trapped fluids to migrate further (England et al., 1987). A detailed site characterization, along with early detection of leaks using technologies capable of detecting small fluid affects in both the reservoir and overburden will support CCS strategies in the future (Eiken et al., 2011; Raef et al., 2005).

Changes in subsurface fluid distribution in time and space modify bulk seismic properties of a medium in four dimensions (4D) (Gassmann, 1951; Mavko et al., 1995; Mavko et al., 2020). Such changes in seismic properties may be sufficiently large to create anomalies in time-lapse seismic data (i.e., seismic reflection data recorded at different times in the same area). Conventional time-lapse seismic data is essential in monitoring subsurface deformation and fluid movement for offshore exploration and production (E&P) industry and CCS operations (Johnston, 2013). Time-related seismic anomalies help identify fluid saturation or pressure changes, potential leakage pathways, microseismic events, and provide information about the structures and properties of the reservoir, seal, and overburden (Souza et al., 2019). Resolution of the seismic image is largely dependent on the frequency bandwidth of the seismic signal, whereby higher frequencies result in better resolved layers and anomalies but with shallower signal penetration, whereas lower frequencies result in greater penetration depth but decreased resolution (Carcione et al., 1988; Lebedeva-Ivanova et al., 2018). As a 4D monitoring tool, high-resolution (high frequency) systems, such as P-Cable, aim to give a very detailed image of pore-fill changes within subsurface depths of 1-2 km (Smith and Mattox, 2020; Waage et al., 2018).

High-resolution imaging of the shallow subsurface has long been a sphere of interest dedicated predominantly to academic research, with the E&P industry focussing resources and technology development towards deep reservoir targets. The increasing focus upon shallow fluid systems (e.g., James et al. (2016)) and geohazards (e.g., Yonggang et al. (2016)) related to current climate change, has resulted in high-resolution seismic acquisition systems being developed with a focus on cost-effective, easy-to-deploy systems that provide high-quality imaging of shallow targets. Such high-resolution data sets generally integrate better with fluid migration modelling studies than conventional data (Souza et al., 2019). The high-resolution P-Cable 3D seismic system is one such acquisition technology that has been utilized to study shallow subsurface gas hydrate fluid flow systems (e.g.

Brookshire Jr et al., 2015; Bünz et al., 2005; Crutchley et al., 2011; Eriksen* et al., 2015; Petersen et al., 2010; Planke et al., 2009; Plaza-Faverola et al., 2010). Continued development of the P-Cable acquisition system and processing software have led to the improvement of data quality and processing techniques tailored to the acquisition system (Eriksen* et al., 2015).

The application of P-Cable 3D seismic data for monitoring fluid related changes (4D) in the shallow subsurface is somewhat recent; initial results of monitoring studies were first published by Waage et al. (2018). Potential target areas for time-lapse P-Cable data are CO_2 storage sites, shallow hydrocarbon prospects, geohazard sites, and fluid flow sites.

The necessity of high-resolution subsurface monitoring is becoming more and more apparent. In this study, we analyse in detail the feasibility of the P-Cable technology as a time-lapse tool for the detection of CO_2 leakage. We introduce the P-Cable 3D seismic technology, summarize and examine the benefits and limitations of the P-Cable seismic system as a monitoring tool, and perform a sensitivity analysis of CO_2 changes on 4D P-Cable seismic data. The sensitivity analysis is conducted using a case study of P-Cable time-lapse data where we (1) model the effect of CO_2 saturation changes on seismic properties, and (2) evaluate the amount of CO_2 change needed to seismically detect an anomaly.

The P-Cable 3D seismic technology

The P-Cable 3D seismic system is a flexible and versatile acquisition system that can be rapidly deployed from small vessels. The system consists of a seismic cable towed perpendicular (cross cable) to the vessel's steaming direction, and up to 24 multi-channel short streamers (25-100 m) are attached to the cross cable (Planke et al., 2009). A standard P-Cable setup consists of 14 streamers of 25 m length, each with 8 receiver groups and separated by 1 meter (Figure 1). Receiver positions are typically calculated using a catenary line equation (Crutchley et al., 2011) constrained by the known length of the cross cable and GPS positions located on each of the two paravanes that extends the cross cable. The system images the shallow stratigraphy with a 6.25 x 6.25 m or 3.12 x 3.12 m bin-size and obtains frequencies up to 500 Hz. The P-Cable technology has proven imaged data quality, surpassing conventional 3D and equal to or better than HiRes 2D (e.g., Brookshire Jr et al., 2016; Meckel and Mulcahy, 2016). The increase in lateral resolution compared to conventional 3D seismic data is approximately one order of magnitude (comparison in Bellwald et al. (2019)). The P-Cable technology images shallow (up to 1-2 km subsurface depths) marine sediments in high detail, where conventional seismic data are typically noisy and of lower resolution. Furthermore, conventional and high-resolution seismic can be combined to optimize the image of shallower and deeper parts of an area (using an approach developed to match seismic images of different resolutions) (Greer and Fomel, 2018). Hence, the technology complements conventional 3D seismic data.

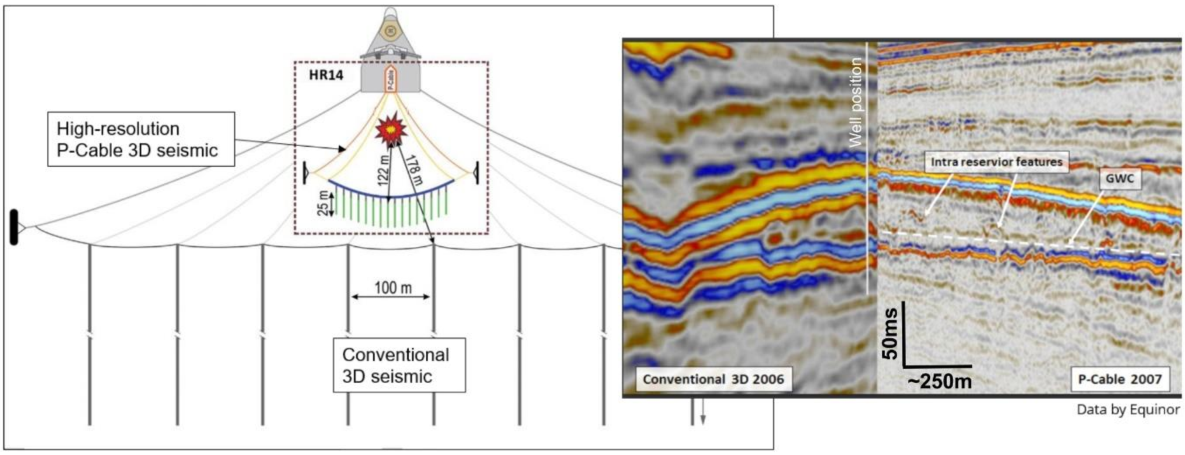

***Figure 1**: Comparison of high-resolution P-Cable and conventional 3D seismic system layout and resolution. The figure is modified after Lebedeva-Ivanova et al. (2018) and www.pcable.com*

P-Cable as a 4D seismic technology

Repeatability of seismic surveys is commonly measured by the normalized RMS (NRMS) of the seismic amplitude difference between the time-surveys (Kragh and Christie, 2002). The NRMS can range between 0 and 200%, where 0% NRMS indicates identical surveys and 200% NRMS indicates surveys that are phase-reversed to each other. The definition of good repeatability for conventional marine (towed-streamer) seismic surveys has improved through time from NRMS values of 40-60% ~10 years ago (Lumley, 2010) to today, where good repeatability typically hasvalues of 20-30% (Landrø and Amundsen, 2018). Values below 20% are considered to be excellent and only possible under optimal 4D acquisition and processing conditions (Landrø and Amundsen, 2018; Lumley et al., 2015).

To be applicable as a time-lapse tool, HR3D time-lapse data must show a good repeatability. So far, time-lapse studies of HR3D seismic data such as the P-Cable technology have been conducted in the Arctic (the Barents Sea, a Northern Norway fjord, offshore Svalbard), the Gulf of Mexico, and offshore Japan.

The first study using P-Cable high-resolution seismic data in a time-lapse series was acquired by UiT – The Arctic University of Norway, using a standard P-Cable setup as described above and two mini GI guns as source with a total volume of 30 in^3 (Waage et al., 2018). A baseline and a repeat survey were collected from three areas with 1-2 years separation. Two sites (site1 and site2) were test-sites (assuming no fluid flow) and one site (site3) was an active seepage site. The sites are characterized by glacial to glaciomarine sediments in a Norwegian fjord (site1), glacial till and Cenozoic sedimentary rocks in the overburden of a CO_2 storage site (the Snøhvit field in the Barents Sea; site2), and a natural seepage and gas hydrate system in a deep-water contourite drift offshore western Svalbard (Vestnesa

Ridge; site3). These three sites of early HR4D P-Cable seismic data (Waage et al., 2018) show comparable NRMS values (~30-40%) to conventional seismic data, although the NRMS measure worsens with high-frequency content (Burren and Lecerf, 2015). Among these the Arctic sites, geometric repetition accuracy of source- and receiver positions was good (<6.25-10 m), and the source signal was well repeated (Waage et al., 2018). A distinguishable difference in repeatability varied dependent on surface conditions, trace fold (the amount of traces in each bin), shot interval at the deep-water Vestnesa Ridge, and the type of sediments or sedimentary rocks imaged. Static trace variations induced by surface conditions such as waves and tides introduced the most significant non-repeatability, thus static corrections in the 4D processing routine were very important to improve repeatability. Higher trace densities resulted in better repeatability due to the increased signal-to-noise ratio. The introduction of noise from previous shots decreased repeatability at the ~1200 m deep-water site. Therefore, optimal shot interval and consequently trace density should be evaluated on future P-Cable data in deep-water fields (Waage et al., 2018). Subhorizontal marine sedimentary deposition also showed good repeatability (NRMS values of 28-30%) compared to areas with complex geology (NRMS values of ~40-70%) that have potential for seismic energy scattering, such as moraine ridges and rough glacial surfaces. However, the difference data show only minor differences along these chaotic reflections, indicating that the processing routine has adequately accounted for most effects of scattering energy and diffraction collapse during migration. The seismic chimneys associated with active seepage at Vestnesa Ridge contained pockets of time-lapse anomalies. These are potentially real fluid related changes as fluid migration is anticipated through an actively seeping chimney. The layered stratigraphy between the chimneys as well as some known carbonate deposits in the shallow subsurface showed little anomalies and high repeatability (NRMS ~ 30%).

Typical P-Cable seismic data has a 6.25 x 6.25 m^2 or 6.25 x 3.125 m^2 bin size and of 2-4 m vertical resolution in the shallow subsurface (Eriksen* et al., 2015; Petersen et al., 2010; Smith and Mattox, 2020; Waage et al., 2018). A recent estimate based on a theoretical study of seismic wave propagation (Lebedeva-Ivanova et al., 2019) shows that the upper part (<600 m) of the subsurface can potentially be resolved with a 1 m resolution in both horizontal and vertical directions using a P-Cable 3D seismic system. To obtain such fine scales, Lebedeva-Ivanova et al. (2019) suggest that essential acquisition factors are: (1) the spectrum of the seismic source must contain frequencies up to 600 Hz, (2) the source-receiver distance must be below 200 m, and (3) the trace density must exceed 4 traces per square meter (78 traces per bin assuming 6.25 x 3.12 m bin size). To test the theoretical analysis, Bellwald et al. (2018) re-binned P-Cable 3D seismic data of Vestnesa Ridge offshore Svalbard and the Snøhvit field in the Barents Sea (time-lapse data presented in Waage et al. (2018)) to 6.25 x 3.125 m and reprocessed with improved vertical and horizontal resolution. The reprocessed data from the Vestnesa Ridge show, for example, a vertical resolution of <1 m from the seabed and to 50 m below, and 1 m resolution between 50 and 150 m below the seafloor. The increase in resolution leads to the detection of small layers and faults within and between the gas chimneys.

In the Gulf of Mexico, time-lapse P-Cable data have been acquired at two deep-water sites (Hatchell et al., 2018; Hatchell et al., 2019; Smith and Mattox, 2020) and a test of P-Cable time-lapse repeatability was conducted in 2014 (Smith and Mattox, 2020). The repeated survey consisted of two sail-line repeats right after a larger P-Cable 3D seismic survey was conducted. The acquisition was done using 100 m long streamers and a source of 201 in^3. The geometric accuracy was high and similar to the studies conducted in the Arctic and minimal time between the surveys likely limited the environmental- and acquisition related differences, contributing to impressively low NRMS values of 10-30% (below 10% for frequencies between 40 and 150 Hz and 10-30% for on frequencies between 130 and 250 Hz). The best signal-to-noise ratio is present within 130 to 250 Hz range, and these frequencies show somewhat larger NRMS values due to the high-frequency content. The study concludes that the acquisition system is well-suited for seismic monitoring the shallow subsurface (less than 1-2 km below the seafloor).

A more recent P-Cable time-lapse campaign in the Gulf of Mexico presents the broadband 4D processing flow (Hatchell et al., 2018) and time-lapse data (Hatchell et al., 2019). The baseline and repeat surveys were acquired 1 year apart in 2016 and 2017 using a 300 in^3 source array and 16-18 100 m long streamers, targeting two reservoirs at subseafloor depths of 1700 m and 2800 m (Hatchell et al., 2019). Hatchell et al. (2019) demonstrate very good repeatability (NRMS ~10-30%) and identify hardening associated with water replacing oil around injection wells. They furthermore suggest number of improvements to the method that further reduce the difference, such as shooting with a larger source to improve SNR, tow source and receivers deeper to increase the low frequency response, improve receiver isolation to reduce strumming noise from the cross cable and place the source behind or outside on the sides of the receiver spread to reduce the effects of the source-bubble.

A study conducted offshore Japan (Meckel et al., 2019), presents time-lapse data of high-resolution seismic acquired using four geo-streamers (and no cross cable), and suggest that high-resolution P-Cable 3D seismic have the potential for excellent repeatability here, and P-Cable time-lapse surveys are planned in the future. The study also presents a broadband processing flow intended to increase repeatability, which can be considered as a future processing guide for P-Cable time-lapse data.

Data and methods

We test the sensitivity or detectability of changes in CO_2 saturation through 4D P-Cable seismic data using rock physics and seismic modelling of P-Cable time-lapse data from the Snøhvit CO_2 storage site as a case example. Two high-resolution P-Cable 3D seismic cubes, a baseline survey (2011) and a monitoring survey (2013), were acquired at the Snøhvit field located in the Hammerfest Basin in the western Barents Sea (Figure 2). Here, glacial tills dominate the stratigraphy down to ~50 m below the seafloor (~442 ms TWT). Below, an interval of ~410 m of westward dipping sedimentary clinoforms, the Torsk Formation of Palaeocene-Eocene age, are characterized by non-calcareous claystones (Figure 2) (Tasianas et al., 2018). These two units are separated by the upper regional unconformity (URU) which is commonly seen as a high-amplitude reflection separating glacial from pre-glacial units across the Barents Sea (Bellwald et al., 2019). The data contains frequencies between 20 and 375 Hz and were processed according to established 4D processing routines (Waage et al. 2018), with the Torsk Fm. as the focus area (initial scaling and trace-by-trace static shift targeted on 200-300 ms).

All horizons within the Torsk Fm. are well-repeated (Figure 2D) and show an average NRMS of ~0.3 (Figure 2D), within the limits of good repeatability as per industry standards. The Nordland Gr. shows somewhat poorer repeatability, but this is partly related to 4D calibration steps focused on the Torsk Fm. Lower repeatability typically occurs across rough topographic landforms such as pockmarks and glacial lineations (Waage et al., 2018). Along horizon T625 (Figure 3), located at ~500 mbsl, the maximum seismic amplitude of the difference seismic is <18% of the seismic amplitude along the same horizon in the baseline/repeat seismic. This 4D signal-noise ratio is representative of the entire unit (Figure 2). Thus, we consider 18 % acoustic impedance contrast as the maximum 4D seismic noise level, and any subsurface changes that produce an acoustic impedance contrast larger than this to be seismically detectable.

To evaluate the detectability of small pore-fill changes on P-Cable 3D seismic time-lapse data in the overburden of the Snøhvit field, we (1) quantified the time-lapse noise between the surveys, (2) performed a theoretical sensitivity analysis to find anticipated changes in acoustic impedance when CO_2 replaces saltwater in pore-spaces at a certain depth, and (3) compared this analysis with the non-repeatable noise on the two time-lapse sets presented by the case study.

We analysed acoustic impedance contrast changes with changes in CO_2 saturation along horizon T625 within the Torsk Fm. (Figures 3 and 4). Rock properties were obtained from well 7121/7-1 at 167 m subseafloor depth in the Snøhvit field area (Torsk Fm.). The non-calcareous claystones of the Torsk Fm. contain predominantly clay (90%) and some quartz (10%) (Dalland et al., 1988). We used 30% porosity and 2100 m/s as a background seismic velocity of water saturated sediments. Bulk properties of CO_2 at 167 m depth below the seafloor are estimated using the approach of Batzle and Wang (1992). Pressure and temperature required to determine fluid bulk properties using Batzle and Wang (1992) were calculated using 4.5°C as the water temperature at the seafloor and a geothermal gradient of 35°C/km. We mixed CO_2 with brine inside the pore spaces to estimate effect of CO_2 on bulk seismic properties assuming homogenous (using Reuss bounds) and patchy (using Voigt bounds) CO_2 distribution in pore spaces (Mavko et al., 2020). The Gassmann (1951) theory was used for fluid substitution to estimate effective bulk properties in this case under different CO_2 saturations. We used a noise level cut-off of 18%, which effectively considers 4D noise, as well as seismic detectability parameters.

We performed a seismic modelling study using the software SeisRoX^{TM} (which uses the approach of Georgsen and Kolbjørnsen (2008)) to evaluate seismic amplitude changes at different CO_2 saturations using our high-resolution 4D seismic data. We picked 8 layers and use porosity and density well logs from nearby well 7121/7-1 to generate background synthetic seismic data (Figures 4A-B). Another synthetic seismic data was then generated assuming homogeneous CO_2 gas distribution with variable gas saturation along a layer below horizon T625. Differences in seismic amplitude due to CO_2 saturation were then added to 4D seismic difference data (Figures 2C and 4D). A proper scaling factor was derived using an RMS level of reflection amplitudes in synthetic data (Figure 4B) and 4D baseline seismic survey (Figure 4A).

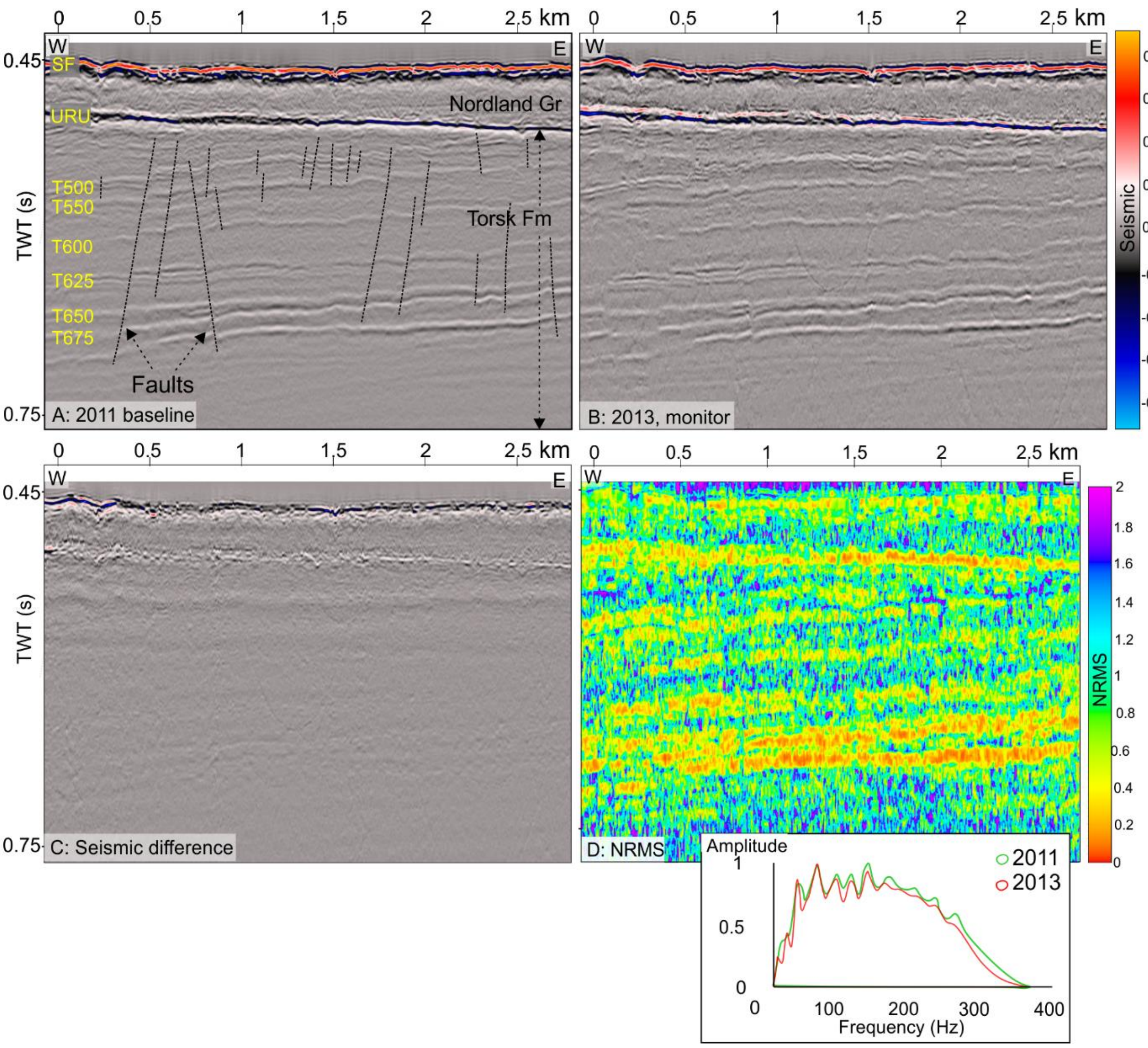

__Figure 2.__ Time-lapse example of P-Cable data acquired in the Snøhvit field showing an inline of the baseline (A), monitor (B),the difference between monitoring and baseline survey data (C),and the comparable NRMS section using 5 ms running interval (D). Small faults strike through the formation

offsetting the horizons slightly. The difference data within the Torsk Fm. show anomalies below 18% of the maximum seismic amplitude, which we set as the time-lapse noise-threshold, since the area is regarded as "quiet" in terms of fluid flow (meaning that the area does not show indications of subsurface fluid flow or seafloor seepages according to available and published data; Waage et al. (2018)).

Sensitivity analysis on 4D P-Cable seismic data

The presence of fluids in the pore spaces of sediments plays an important role in the effective bulk seismic properties of a medium (Gassmann, 1951; Mavko et al., 1995; Mavko et al., 2020). Injection of CO_2 in a sequestration formation decreases the seismic velocity and fluid density, while leakage would deplete the gas in the formation and lead to an increase in seismic velocity and fluid density. Changes in acoustic impedance due to variations in seismic velocity and density at a reservoir level create 4D anomalies in time-lapse seismic data. Thus, injection, leakage and movement of CO_2 gas in the subsurface can be quantitatively assessed by investigating changes in seismic velocity and acoustic impedance. However, spatial heterogeneity, resolution and uncertainties (e.g. repeatability) of the reservoir or overburden affect the accuracy of monitoring (Daley et al., 2011).

Due to their high frequency content and spatial resolution, P-Cable time-lapse datasets are expected to resolve fluid changes on a very small scale (1-5 m) and at lower saturations; thus, we expect that the high-resolution P-Cable technology can better resolve different modes of subsurface fluid movements than conventional time-lapse seismic data. It is further to note important that the 4D anomalies created by the movement of CO_2 gas in the subsurface must exceed the non -repeatable noise level between the time-lapse pairs in order to detect CO_2 movement (Meckel et al., 2019).

As predicted by theoretical and applied work (Gassman, 1951; Mavko et al., 2020; Mukerji and Mavko, 1994; Shi et al., 2007), the P-wave velocity and P-wave acoustic impedance decreases with increasing CO_2 in pore spaces (Figure 3). The two end members of fluid distribution in a medium, which depend on the heterogeneity of the medium, are homogenous and patchy. Assuming a homogenous saturation, the analysis shows that a reduction in P-wave impedance of 18% (noise-limits) represent a minimal H_2O - CO_2 exchange of only 3.3% of available pore spaces (Figure 3B). If the saturation is patchy, our analysis indicates that the same reduction in P-impedance represents an H_2O - CO_2 exchange of 27.4% (Figure 3B). However, the detection ability of partial leakages decreases at higher CO_2 saturations, under a homogeneous gas distribution assumption (Figure 3B). For example, a change in CO2 saturation from 0 to 3.3% (3.3%) will create almost the same effect on 4D seismic difference as a change from ~8 to 21% (13%) in CO2 saturation (Figure 3B). The effect of CO_2 saturation changes on the seismic data is relatively uniform when the distribution is patchy. .However, a 100% water-saturated medium would require a substitution of 27.4% of CO_2 to overcome the noise-threshold (Figure 3B). Thus, CO_2-saturation changes above ~3.3-27.4% can, in theory, be detected on these time-lapse data depending on how the fluid is distributed in pore spaces.

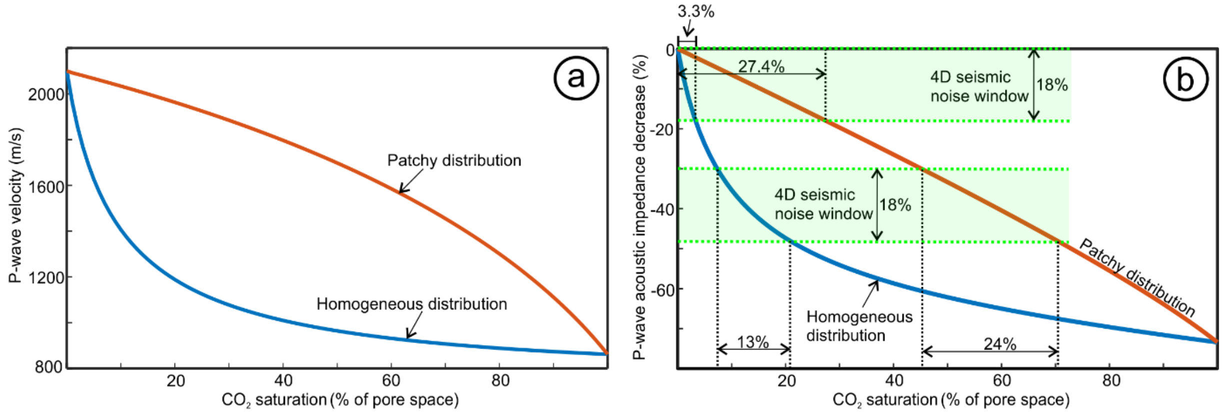

Figure 3. *The variation in the P-wave velocity (A) and the relative decrease in the P-wave acoustic impedance in % (B) as a function of CO_2 saturation in pores for homogenous (blue line) and patchy (red line) saturation of non-calcareous claystones with 30 % porosity (further rock properties are described in the method chapter). The green lines show noise windows and dotted black lines indicate the changes in CO_2 saturation needed to surpass the noise thresholds and therefore be seismically detectable on high-resolution P-Cable time-lapse seismic data. The 4D noise window showing a decrease in acoustic impedance from 0 to 18% highlights a complete CO_2 leakage scenario (initially no CO_2 in pore spaces) whereas the noise window showing decrease in acoustic impedance from 30% to 48% shows a partial CO_2 leakage scenario (some CO_2 is initially present in pore spaces).*

The synthetic seismic data show the effect of the presence of CO_2 at different saturations (Figures 4C-D). Looking at the layer between T625 and T650 in the synthetic data (Figure 4C+D), at one location the synthetic data assume an area with saturation values of CO_2 ranging from 0 to 80% and at another location, a stable CO_2 saturation of 3.3%. The latter creates changes in seismic data that are above the 4D noise level and can be clearly observed in the 4D seismic data (Figure 4D). However, the 4D noise is different from fluid anomalies as can be seen from results obtained through seismic modelling (Figure 4D), thus, actual CO_2 detection limits will be lower if the anomaly is larger (Chadwick et al., 2014).

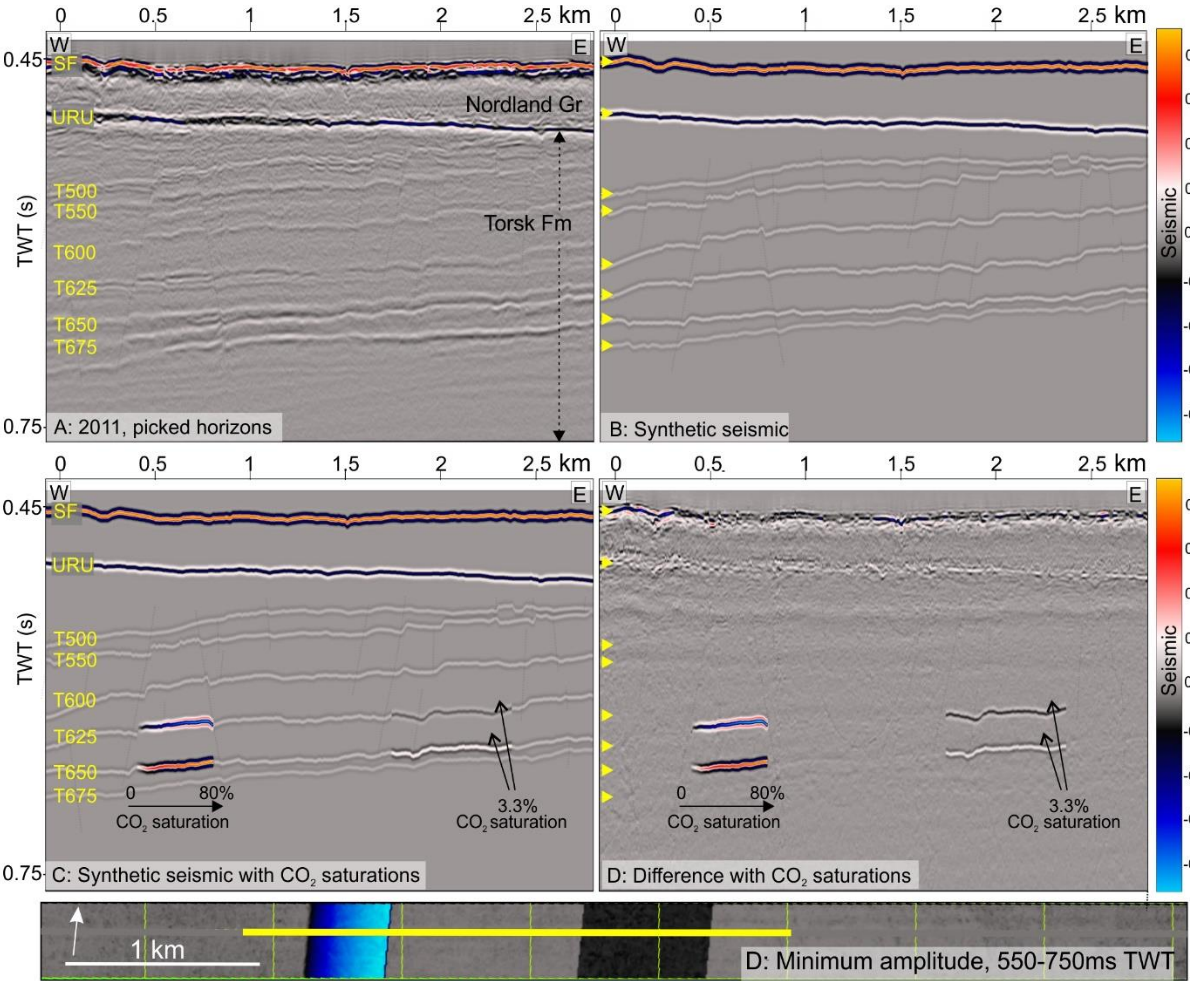

Figure 4. *Time-lapse example of P-Cable data acquired in the Snøhvit field showing an inline from the baseline survey with indication of picked horizons (yellow text (A,C) and arrows (B,D). (A), synthetic seismic (B), the synthetic seismic with anomalies as result of CO_2 accumulations (C), and the difference section combined with the CO_2 anomalies (D). The lower map shows the maximum negative amplitude in volume D between 550 and 750 ms (0-0.18) The yellow line show location of seismic profile (A-C); whereas the black patch represent a 3.3% CO_2 saturation anomaly (assuming homogenous distributed gas), and the black-blue patch a 0-80% saturation CO_2 anomaly.*

Assuming changes in CO2 saturation equal to the detection limits found above, distributed in a small volume of seismic data equal to the three-dimensional resolution (6.25 x 6.25 m (bin size) x 5 m (conservative vertical resolution) = 195 m^3), we calculate that ~2-16 m^3 of CO_2 can, in theory, be detected. This equals 1,320-10,560 kg or ~1.3-10.6 tonnes of CO_2 distributed over a small volumeof 195 m^3. An example of the calculation is shown below.

Volume occupied by CO_2 assuming 30% porosity and 3.3% saturation (homogenous):

$$195\ m^3 x(0.3 \times 0.033) \approx\ 2\ m^3$$

Volume converted to weight assuming a CO_2 density of 660 kg/m^3 (Batzle and Wang, 1992):

$$2\ m^3\ x\ 660\ \frac{kg}{m^3} = 1320\ kg\ or\ {\sim}1.3\ tonnes\ of\ CO_2$$

A previous study (Chadwick et al., 2014) attempted to estimate the amount of CO_2 gas leakage required to be detectable in conventional time-lapse seismic data. Chadwick et al. (2014) calculated detection limits of CO_2 in the overburden of the Sleipner field offshore Norway at similar depths (490 m) using conventional time-lapse data. According to that study, large CO_2 anomalies (>70,000 m^2) are detectable if they exceed ~20% change in acoustic impedance and small anomalies (~156 m^2) need to exceed a change in acoustic impedance of 80% to be detectable (with a 100% probability). The study furthermore converts the detection thresholds to CO_2 amounts using a conservative end member of fully saturated CO_2 in pore spaces. To exceed the detection thresholds of these conventional seismic data, 315 tonnes of CO_2 must have leaked into the overburden to be detected. Differences in the horizontal and vertical resolution in P-Cable seismic data and conventional seismic create big differences in the detectable amount of CO_2 (1.3-10.6 t versus 315 t, respectively).

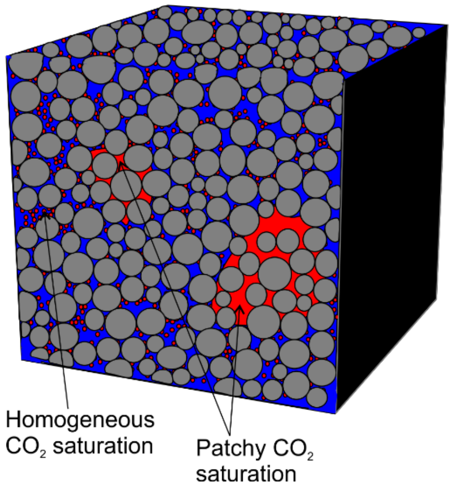

Figure 5. *CO_2 distribution types in sediment or sedimentary rocks: CO_2 can be distributed patchy, homogeneous, or as a mixture of the two.*

Discussion

Sensitivity of high-resolution P-Cable seismic to CO_2 changes in the subsurface

High-resolution P-Cable 3D seismic has a much better vertical resolution than conventional seismic data and increase in lateral resolution is up to one order of magnitude (Bellwald and Planke, 2019; Planke et al., 2009). The advantages of P-Cable seismic data are enhanced due to the role that vertical resolution plays in detecting small structures or fluid accumulations in the subsurface, e.g. CO_2 in thin layers and generally smaller heterogeneities. A number of studies also (Bellwald et al., 2019; Bellwald et al., 2018; Lebedeva-Ivanova et al., 2019) show that the P-Cable seismic system is able to resolve shallow features at ultra-high resolution (≤1 m), therefore the potential of P-Cable seismic as an ultra-high resolution 4D monitoring tool should be evaluated. Smaller bin sizes, required for ultra-high resolution, will however contribute to lower fold, which generally reduces the signal-to-noise ratio, and thus the repeatability (Waage et al., 2018). Traces can be regenerated by interpolation and regularization, however this will also affect repeatability. Gaps in the raw bins increase the risk of non-repeatable sources in the data (Meckel et al., 2019; Waage et al., 2018), hence, there must be a careful consideration of the optimal processing parameters and steps to eventually generate the highest possible repeatability. However, the flexibility of the P-Cable system enables tailoring of the acquisition layout (optimized positioning systems and acquisition parameters (i.e. number of streamers, streamer- and receiver spacing, size and number of sources)) for the target depth and resolution. Nevertheless, if seismic data can image meter-sized objects repeatedly, 3D and 4D characterization have a potential orf reliable quantitative property analysis of the subsurface (Lebedeva-Ivanova et al., 2019).

The depth at which a CO_2 reservoir can be imaged with P-Cable 3D and 4D data naturally varies with the size of source and length of the streamers. The water depth, geology and the potential presence of shallow gas also act as major controls on P-Cable imaging depth. One of the deepest examples of P-Cable imaging is reported in the publication of Hatchell et al. (2019) which show that using 100 m long streamers and a 300 in^3 source array, good imaging and high repeatability of P-Cable time-lapse data is achieved at 2.5-3 km subseafloor depths. Some examples of other sites with the potential of good imaging at great depths are likely offshore West Africa and offshore Brazil (Smith and Mattox, 2020).

There are significant differences in seismic detection ability depending on the CO_2 distribution in the subsurface. At low saturations (< 10%), changes in CO_2 that are uniformly spread in the subsurface are easier to detect than in CO_2 occurring in patches. The distribution of CO_2 is patchy when the size of CO_2 accumulation in pore spaces becomes comparable to the wavelength, and assumed to be homogeneous if the patch size is much smaller than the size of wavelength (Azuma et al., 2013). Wavelengths in P-Cable seismic data are lower than conventional seismic data, typical in the range of 5-20 m compared to ~20-225 m. Hence, a patchy CO_2 distribution in P-Cable seismic data may be defined as homogeneous distribution in a conventional seismic dataset. In a practical sense, the patch size to consider the CO_2 distribution homogenous may be 4-5 times smaller on P-Cable time-lapse. Regardless, depending on CO_2 distribution and CO_2 patch sizes, uncertainties around the fluid distribution type may limit some of the gains in seismic detectability obtained from improved vertical resolution. Many studies of conventional time-lapse data anomalies lean on a spectre of partial patchy saturation fluid substitution models (initially proposed by White (1975)) because these models have shown to appear closer to observational data (Daley et al., 2011). Conversely, modelling studies, such as Behzadi et al. (2011) show that using multiphase fluid flow simulations presenting a range of heterogeneities, the Vp-Sw relationship never reaches the patchy model curve (upper bound) even at the highest heterogeneity level in the model.

Choosing the most realistic fluid distribution model for an area or sub-area (saturations may also change within a reservoir) reduce the uncertainties regarding fluid saturations (distribution). Well logs, core data, P- and S-waves data, and surface analogues of the specific formation are i.e. important in identifying causes of fluid heterogeneities such as permeability, porosity, grain-size distribution and contrasts, and sedimentary bedform architecture (i.e., lamina, ripples, cross-stratifications) (Trevisan et al., 2017). A common indication of heterogeneities which may alter the permeability and therefore fluid distribution is variating depositional flow regime leading to stratification and larger grain-size contrasts. In our case study at the overburden of the Snøhvit field, information from the well log and completion report of well 7121/7-1 of the Sotbakken Gr./Torsk Fm show relatively little variations in grain size (gamma ray ~40-60 GAPI) and the depositional environment was interpreted as a marine environment with restricted bottom water circulation, which give the potential for a more homogenous fluid substitution if permeability is effective (Trevisan et al., 2017).

In the case of a real CO_2 storage reservoir, there is a greater likelihood of patchy distributed CO_2 right after the injection process of CO_2 in low permeability sediments (Behzadi et al., 2011; Wisman, 2012). CO_2 distributes more uniformly in pore spaces with time due to diffusion and other processes that homogenise the medium over time. However, faults or self-enhanced vertical fluid flow structures (e.g. chimneys) at shallow depths can act as potential CO_2 leakage pathways and the presence of CO_2 in these structures can exhibit some patchy behaviour depending on the thickness of the fault plane or chimney width. Seismic attenuation is also quite sensitive to the presence of gas and high-resolution P-Cable 3D seismic data is best suited for seismic attenuation estimates in a medium due to its broad bandwidth (Singhroha et al., 2016). Studying time-lapse changes in seismic attenuation has a potential to give further insight into CO_2 distribution modes, including pore-pressure, temperature- and rock frame differences, which might be altered due to the injection of CO_2 and therefore impact the time-lapse anomalies.

The EU CCS Directive (Union, 2009) requires the monitoring of CO_2 storage and the detection of irregularities and leakage at the seafloor and in the subsurface. Various parties including policy makers seem to agree that the only acceptable leakage rate for CO_2 storage in geological layers is zero. However, multiple studies suggest that leakage rates of 0.01% annually or less ensure efficient greenhouse gas mitigation (Hepple and Benson, 2005; Miocic et al., 2019). In the case of the Snøhvit field, 700,000 tonnes of CO_2 are injected annually, and 0.01% is equivalent to 7000 tonnes of CO_2 per year. This amount equals the average CO_2 emissions of 5384 people considering that the global average CO_2 footprint per person is 1.3 tonnes per year (4.5 tonnes a year per person in the USA) (Friedlingstein et al., 2019). Studies on detection limits for conventional seismic data in the overburden of the Sleipner CCS field (offshore Norway) indicate that leakage of 300 tonnes is detectable at comparable depths below the seafloor (Chadwick et al., 2014). This might be a relatively small number, however, P-Cable achieves a high-resolution seismic detection limit of as low as 1.3-10.6 tonnes of CO_2, comparable to the annual average carbon emissions of only one to two people. The difference in leakage detection between these two studies is mainly caused by the difference in seismic resolution. The potential P-Cable detection threshold is much lower than the acceptable leakage rate for injected CO2, so much so that it can detect changes in CO2 saturation that correspond to leakage rates of next to 0%..

CCS operations in the future

Carbon Capture and Storage and seismic monitoring thereof will have a significant role in reducing industrial CO_2 emissions aiming to address future climate targets (Ringrose and Meckel, 2019). The continental margins around the world are the ideal geological targets that can accommodate the large quantities of CO_2 sequestration required to reduce atmospheric levels of CO_2 (Ringrose and Meckel, 2019). It is suggested that the best available storage sites on the continental margins are found in shallow, mainly post-rift Cenozoic stratigraphy (Ringrose and Meckel, 2019). The overburden of such sites is ideal for good imaging of high-frequency (high-resolution) seismic. Thus, high-resolution baseline and site surveys are required for mapping potential overburden leakage migration pathways and shallow gas pockets with high confidence and might be critical during future CCS operations for detailed containment monitoring, especially if leakage is detected from the reservoir level. It is the ability to detect both small changes and the strong response expected for small CO_2 saturations that makes high-resolution 3D seismic ideal for CO_2 containment monitoring. The limited offset range makes key reservoir characterization methods such as AVO analysis challenging or impossible. In addition, broad frequency bandwidth up to 400 Hz imposes depth restrictions and limited undershooting possibilities. However, P-Cable is a flexible, versatile and cost-efficient high-resolution 3D seismic system that ideally supplements conventional 3D seismic for monitoring offshore carbon storage.

The limited studies that exist on high-resolution 3D seismic repeatability indicate that it is well-repeatable (industry-standard NRMS) if the time-lapse surveys are acquired using comparable acquisition and surface conditions (wave height, tides, water currents etc.), survey layout, and acquisition parameters (Hatchell et al., 2018; Meckel et al., 2019; Waage et al., 2018). The number of existing P-Cable time-lapse surveys is low, therefore, we expect that the repeatability will improve with an increased number of surveys as our understanding of the acquisition, processing and geology-related effects on reproducibility increases.

Conclusions

The studies that exist on high-resolution, in particular P-Cable 3D seismic time-lapse data show that this acquisition technology is able to obtain good repeatability, indicating a potential for future high-resolution time-lapse seismic. Analysis of the P-Cable data detection limits shows that very small CO_2

saturation changes are detectable in well-repeatable P-Cable data (1.3-10.6 tonnes; 3.3-27.4% gas saturation). The results indicate that the system is capable of recognizing very small CO_2 leaks, far smaller (approximately two orders of magnitude lower) than conventional seismic data, which is presently the premier monitoring tool for CO_2 storage. Based on our results, we conclude that the P-Cable acquisition system, being a cost-effective method, has the potential to be used in both frontier and mature regions to acquire successive small-size surveys (25-250 km^2) in areas of particular interest, e.g. 4D seismic monitoring of the shallow overburden at CO_2 storage sites that have suspected leakage from the reservoir and supplement conventional time-lapse surveys for monitoring storage site integrity in the future.

Acknowledgements

This work is partly supported by the Research Council of Norway through its Centres of Excellence funding scheme, project 223259 and for SP, project number 223272. The work is also supported by the STEMM-CCS project funded by the European Union's Horizon 2020 research and innovation programme under grant agreement 654462. We thank the crew of *R/V* Helmer Hanssen and those who contributed to P-cable data acquisition. We greatly acknowledge, Schlumberger, CGG (HRS Software), Norsar and Deco Geophysical for providing software and support, and thank Carmen Braun at UiT for proof reading. The data will be stored in the UiT open research data repository.

References

Alcalde, J., Flude, S., Wilkinson, M., Johnson, G., Edlmann, K., Bond, C. E., Scott, V., Gilfillan, S. M. V., Ogaya, X., and Haszeldine, R. S., 2018, Estimating geological CO2 storage security to deliver on climate mitigation: Nature Communications, v. 9, no. 1, p. 2201.

Azuma, H., Konishi, C., and Xue, Z., 2013, Introduction and application of the modified patchy saturation for evaluating CO2 saturation by seismic velocity: Energy Procedia, v. 37, p. 4024-4032.

Batzle, M., and Wang, Z., 1992, Seismic properties of pore fluids: Geophysics: Geophysics, v. 57, p. 1396-1408.

Behzadi, H., Alvarado, V., and Mallick, S., 2011, CO2 saturation, distribution and seismic response in two-dimensional permeability model: Environmental science & technology, v. 45, no. 21, p. 9435-9441.

Bellwald, B., and Planke, S., 2019, Shear margin moraine, mass transport deposits and soft beds revealed by high-resolution P-Cable three-dimensional seismic data in the Hoop area, Barents Sea: Geological Society, London, Special Publications, v. 477, no. 1, p. 537-548.

Bellwald, B., Planke, S., Lebedeva-Ivanova, N., Piasecka, E. D., and Andreassen, K., 2019, High-resolution landform assemblage along a buried glacio-erosive surface in the SW Barents Sea revealed by P-Cable 3D seismic data: Geomorphology, v. 332, p. 33-50.

Bellwald, B., Waage, M., Planke, S., Lebedeva-Ivanova, N., Polteau, S., Tasianas, A., Bünz, S., Plaza-Faverola, A., Berndt, C., and Stokke, H., Monitoring Of CO2 Leakage Using High-Resolution 3D Seismic Data–Examples From Snøhvit, Vestnesa Ridge And The Western Barents Sea, *in*

Proceedings Fifth CO2 Geological Storage Workshop2018, Volume 2018, European Association of Geoscientists & Engineers, p. 1-5.
Brookshire Jr, B. N., Landers, F. P., and Stein, J. A., 2015, Applicability of ultra-high-resolution 3D seismic data for geohazard identification at mid-slope depths in the Gulf of Mexico: Initial results: Underwater Technology, v. 32, no. 4, p. 271-278.
Brookshire Jr, B. N., Lippus, C., Parish, A., Mattox, B., and Burks, A., 2016, Dense arrays of short streamers for ultrahigh-resolution 3D seismic imaging: The Leading Edge, v. 35, no. 7, p. 594-599.
Burren, J., and Lecerf, D., Repeatability measure for broadband 4D seismic, *in* Proceedings 77th EAGE Conference and Exhibition 20152015, Volume 2015, European Association of Geoscientists & Engineers, p. 1-5.
Bünz, S., Mienert, J., Bryn, P., and Berg, K., 2005, Fluid flow impact on slope failure from 3D seismic data: a case study in the Storegga Slide: Basin Research, v. 17, no. 1, p. 109-122.
Carcione, J. M., Kosloff, D., and Kosloff, R., 1988, Wave propagation simulation in a linear viscoacoustic medium: Geophysical Journal International, v. 93, no. 2, p. 393-401.
Chadwick, R. A., Marchant, B. P., and Williams, G. A., 2014, CO2 storage monitoring: leakage detection and measurement in subsurface volumes from 3D seismic data at Sleipner: Energy Procedia, v. 63, p. 4224-4239.
Crutchley, G. J., Berndt, C., Klaeschen, D., and Masson, D. G., 2011, Insights into active deformation in the Gulf of Cadiz from new 3-D seismic and high-resolution bathymetry data: Geochemistry, Geophysics, Geosystems, v. 12, no. 7.
Daley, T. M., Ajo-Franklin, J. B., and Doughty, C., 2011, Constraining the reservoir model of an injected CO2 plume with crosswell CASSM at the Frio-II brine pilot: International Journal of Greenhouse Gas Control, v. 5, no. 4, p. 1022-1030.
Dalland, A., Worsley, D., and Ofstad, K., 1988, A lithostratigraphic scheme for the mesozoic and cenozoic and succession offshore mid-and northern norway, Oljedirektoratet.
Eiken, O., Ringrose, P., Hermanrud, C., Nazarian, B., Torp, T. A., and Høier, L., 2011, Lessons learned from 14 years of CCS operations: Sleipner, In Salah and Snøhvit: Energy Procedia, v. 4, p. 5541-5548.
England, W., Mackenzie, A., Mann, D., and Quigley, T., 1987, The movement and entrapment of petroleum fluids in the subsurface: Journal of the Geological Society, v. 144, no. 2, p. 327-347.
Eriksen*, F. N., Berndt, C., Karstens, J., and Crutchley, G., P-Cable High Resolution 3D Seismic-Case Study and Recent Advances, *in* Proceedings Near-Surface Asia Pacific Conference, Waikoloa, Hawaii, 7-10 July 20152015, Society of Exploration Geophysicists, Australian Society of Exploration …, p. 116-119.
Friedlingstein, P., Jones, M., O'sullivan, M., Andrew, R., Hauck, J., Peters, G., Peters, W., Pongratz, J., Sitch, S., and Le Quéré, C., 2019, Global carbon budget 2019: Earth System Science Data, v. 11, no. 4, p. 1783-1838.
Gassman, F., 1951, Über die elastizität poröser medien: Vierteljahrschrift der Naturforschenden Gesellschaft in Zürich.
Gassmann, F., 1951, Über die elastizität poröser medien: Vierteljahrss-chrift der Naturforschenden Gesellschaft in Zurich, vol. 96.
Georgsen, F., and Kolbjørnsen, O., 2008, Simple SIMPLI Inversion.
Greer, S., and Fomel, S., 2018, Matching and merging high-resolution and legacy seismic images: Geophysics, v. 83, no. 2, p. V115-V122.
Hatchell, P., Bakku, S., and Yang, Z., 4D Seismic of deep reservoirs with a low-cost P-cable system, *in* Proceedings 81st EAGE Conference and Exhibition 20192019, Volume 2019, European Association of Geoscientists & Engineers, p. 1-5.
Hatchell, P., Bakku, S., Yang, Z., Lopez, J., Nolan, B., Wang, K., Gee, V., Mestayer, J., King, K., and Scott, L., High-resolution Low-cost 3D and 4D Seismic Surveys for Deepwater Fields, *in*

Proceedings 80th EAGE Conference and Exhibition 20182018, Volume 2018, European Association of Geoscientists & Engineers, p. 1-5.

Hepple, R., and Benson, S., 2005, Geologic storage of carbon dioxide as a climate change mitigation strategy: performance requirements and the implications of surface seepage: Environmental Geology, v. 47, no. 4, p. 576-585.

James, R. H., Bousquet, P., Bussmann, I., Haeckel, M., Kipfer, R., Leifer, I., Niemann, H., Ostrovsky, I., Piskozub, J., and Rehder, G., 2016, Effects of climate change on methane emissions from seafloor sediments in the Arctic Ocean: A review: Limnology and Oceanography, v. 61, no. S1, p. S283-S299.

Johnston, D. H., 2013, Practical applications of time-lapse seismic data, Society of Exploration Geophysicists.

Kragh, E., and Christie, P., 2002, Seismic repeatability, normalized rms, and predictability: The Leading Edge, v. 21, no. 7, p. 640-647.

Landrø, M., and Amundsen, L., 2018, Introduction to exploration geophysics with recent advances, Bivrost.

Lebedeva-Ivanova, N., Polteau, S., Bellwald, B., Planke, S., Berndt, C., and Stokke, H. H., 2018, Toward one-meter resolution in 3D seismic: The Leading Edge, v. 37, no. 11, p. 818-828.

Lebedeva-Ivanova, N., Polteau, S., Zastrozhnov, D., Planke, S., Waage, M., Buenz, S., Bellwald, B., Vanneste, M., Sauvin, G., and Myklebust, R., 2019, Meter-Scale 3D Seismic Data for High-Resolution Site Characterization, v. 2019, no. 1, p. 1-2.

Lumley, D., 2010, 4D seismic monitoring of CO_2 sequestration: The Leading Edge, v. 29, no. 2, p. 150-155.

Lumley, D., Landrø, M., Vasconcelos, I., Eisner, L., Hatchell, P., Li, Y., Saul, M., and Thompson, M., 2015, Advances in time-lapse geophysics—Introduction, Society of Exploration Geophysicists.

Masson-Delmotte, V., Zhai, P., Pörtner, H., Roberts, D., Skea, J., Shukla, P., Pirani, A., Moufouma-Okia, W., Péan, C., and Pidcock, R., 2018, IPCC, 2018: Summary for policymakers: Global warming of, v. 1.

Mavko, G., Chan, C., and Mukerji, T., 1995, Fluid substitution: Estimating changes in Vp without knowing Vs: Geophysics, v. 60, no. 6, p. 1750-1755.

Mavko, G., Mukerji, T., and Dvorkin, J., 2020, The rock physics handbook, Cambridge university press.

Meckel, T., Feng, Y., Treviño, R., and Sava, D., 2019, High-resolution 3D marine seismic acquisition in the overburden at the Tomakomai CO_2 storage project, offshore Hokkaido, Japan: International Journal of Greenhouse Gas Control, v. 88, p. 124-133.

Meckel, T. A., and Mulcahy, F. J., 2016, Use of novel high-resolution 3D marine seismic technology to evaluate Quaternary fluvial valley development and geologic controls on shallow gas distribution, inner shelf, Gulf of Mexico: Interpretation, v. 4, no. 1, p. SC35-SC49.

Miocic, J. M., Gilfillan, S. M., Frank, N., Schroeder-Ritzrau, A., Burnside, N. M., and Haszeldine, R. S., 2019, 420,000 year assessment of fault leakage rates shows geological carbon storage is secure: Scientific reports, v. 9, no. 1, p. 1-9.

Mukerji, T., and Mavko, G., 1994, Pore fluid effects on seismic velocity in anisotropic rocks: Geophysics, v. 59, no. 2, p. 233-244.

Petersen, C. J., Bünz, S., Hustoft, S., Mienert, J., and Klaeschen, D., 2010, High-resolution P-Cable 3D seismic imaging of gas chimney structures in gas hydrated sediments of an Arctic sediment drift: Marine and Petroleum Geology, v. 27, no. 9, p. 1981-1994.

Planke, S., Eriksen, F. N., Berndt, C., Mienert, J., and Masson, D., 2009, P-Cable high-resolution seismic: Oceanography, v. 22, no. 1, p. 85.

Plaza-Faverola, A., Westbrook, G. K., Ker, S., Exley, R. J., Gailler, A., Minshull, T. A., and Broto, K., 2010, Evidence from three-dimensional seismic tomography for a substantial accumulation of gas hydrate in a fluid-escape chimney in the Nyegga pockmark field, offshore Norway: Journal of Geophysical Research: Solid Earth, v. 115, no. B8.

Raef, A. E., Miller, R. D., Franseen, E. K., Byrnes, A. P., Watney, W. L., and Harrison, W. E., 2005, 4D seismic to image a thin carbonate reservoir during a miscible CO_2 flood: Hall-Gurney Field, Kansas, USA: The Leading Edge, v. 24, no. 5, p. 521-526.

Ringrose, P. S., and Meckel, T. A., 2019, Maturing global CO_2 storage resources on offshore continental margins to achieve 2DS emissions reductions: Scientific Reports, v. 9, no. 1, p. 1-10.

Shi, J.-Q., Xue, Z., and Durucan, S., 2007, Seismic monitoring and modelling of supercritical CO_2 injection into a water-saturated sandstone: Interpretation of P-wave velocity data: International Journal of Greenhouse Gas Control, v. 1, no. 4, p. 473-480.

Smith, P., and Mattox, B., 2020, A time-lapse seismic repeatability test using the P-Cable high-resolution 3D marine acquisition system: The Leading Edge, v. 39, no. 7, p. 480-487.

Souza, R., Lumley, D., Shragge, J., Davolio, A., and Schiozer, D., 2019, 4D Seismic Bandwidth and Resolution Analysis for Reservoir Fluidflow Model Applications: ASEG Extended Abstracts, v. 2019, no. 1, p. 1-5.

Tasianas, A., Bünz, S., Bellwald, B., Hammer, Ø., Planke, S., Lebedeva-Ivanova, N., and Krassakis, P., 2018, High-resolution 3D seismic study of pockmarks and shallow fluid flow systems at the Snøhvit hydrocarbon field in the SW Barents Sea: Marine Geology, v. 403, p. 247-261.

Trevisan, L., Krishnamurthy, P., and Meckel, T. A., 2017, Impact of 3D capillary heterogeneity and bedform architecture at the sub-meter scale on CO_2 saturation for buoyant flow in clastic aquifers: International Journal of Greenhouse Gas Control, v. 56, p. 237-249.

Union, E., 2009, Directive 2009/28/EC of the European Parliament and of the Council of 23 April 2009 on the promotion of the use of energy from renewable sources and amending and subsequently repealing Directives 2001/77/EC and 2003/30/EC: Official Journal of the European Union, v. 5, p. 2009.

White, J., 1975, Computed seismic speeds and attenuation in rocks with partial gas saturation: Geophysics, v. 40, no. 2, p. 224-232.

Wisman, P. S., 2012, Rock physics changes due to CO_2 injection: the CO2CRC Otway Project: Curtin University.

Waage, M., Bünz, S., Landrø, M., Plaza-Faverola, A., and Waghorn, K. A., 2018, Repeatability of high-resolution 3D seismic data: Geophysics, v. 84, no. 1, p. B75-B94.

Yonggang, J., Chaoqi, Z., Liping, L., and Dong, W., 2016, Marine geohazards: Review and future perspective: Acta Geologica Sinica-English Edition, v. 90, no. 4, p. 1455-1470.

www.pcable.com?